Eur. Phys. J. Plus (2023) 138:80
https://doi.org/10.1140/epjp/s13360-022-03579-6

THE EUROPEAN PHYSICAL JOURNAL PLUS

Regular Article

A Monte Carlo simulation study on the evaluation of radiation protection properties of spectacle lens materials

Sevim Bilici[1], **Mirac Kamislioglu**[2,3,a], **Elif Ebru Altunsoy Guclu**[4,5]

[1] Department of Opticianry, Vocational School of Health Services, Bandirma Onyedi Eylul University, Balıkesir, Turkey
[2] Department of Medical Imaging Techniques, Vocational School of Health Services, Bandirma Onyedi Eylul University, Balıkesir, Turkey
[3] Boron Technologies Application and Research Center (BORTAM), Bandirma Onyedi Eylul University, 10200 Balıkesir, Turkey
[4] Department of Medical Imaging Techniques, Vocational School of Health Services, Uskudar University, Istanbul, Turkey
[5] Medical Radiation Research Center (USMERA), Uskudar University, 34672 Istanbul, Turkey

Received: 16 July 2022 / Accepted: 7 December 2022

Abstract The eye lens has been known a radiosensitive tissue. Radiation exposure can cause opacities, cataracts and vision loss. The sensitivity of the eyes to ionizing radiation has attracted attention in the last decade. ICRP announced that equivalent dose limit of eye lens has dropped in recent years. Therefore, spectacle lens selection is becoming increasingly important. In this study, the radiation protection properties of spectacle lens (CR-39, Polycarbonate and Trivex) materials were investigated using the MCNP-6.2 Monte Carlo code and SRIM software. The suitability of the results obtained with MCNP-6.2 Monte Carlo code was provided by comparing the theoretical results obtained from the WinXCOM program. The results showed that the CR-39 spectacle lens had minimum half-value layer, tenth value layer and mean free path values. In addition to the photon protection properties of spectacle lens materials, proton (H^{1}) and alpha (He^{+2}) radiation protection properties were also investigated. Mass stopping power and projected range (PR) values for proton and alpha particles were calculated using SRIM code in the energy range of 0.01–10 MeV. As a result of the research, it was seen that the CR-39 lens had minimum PR values.

1 Introduction

Spectacle lenses are undoubtedly one of the most basic requirements for a better quality of life in people with vision problems. According to the World Health Organization (WHO), currently, at least 1 billion of the approximately 2.2 billion people worldwide have a vision impairment that can be prevented or yet to be addressed [1]. This situation is proportional to the demand for the spectacle lenses to be used. The importance of using spectacle lenses increases both in different age groups and in people who can see with only one eye. In addition, it should not be overlooked that spectacle lenses are used not only by people who have problems with vision but also by people who wear sunglasses. It is clear from such situations that spectacle lenses appeal to many areas. In this study, the radiation protection properties of spectacle lens (CR-39, Polycarbonate, Trivex) materials were investigated. These spectacle lenses selected in our study are lighter and have higher impact resistance compared to other spectacle lenses due to the chemical structure and composition of the materials in their structure. Especially Polycarbonate lenses have an excellent impact resistance. Trivex is highly preferred in daily life [2]. CR-39 (Columbia Resin) lens developed by Pittsburgh Plate Glass Company (PPG) is also known as allyl diglycol carbonate. Made of CR-39 monomer, the lenses are resistant to scratches, heat and household chemicals [2–4]. Polycarbonate was developed by General Electric (GE) Corporation and named Lexan. Polycarbonate is another milestone in the development of optical polymers. Polycarbonate spectacle lenses consists of Bisphenol A. For this reason, Bisphenol A is also called Polycarbonate. Polycarbonate has advantages such as low density and high impact resistance and high abbe value compared to CR-39 [5]. On the other hand, in 2001 PPG focused on Trivex lenses, which have impact resistance comparable to Polycarbonate but are lighter materials. Trivex lenses were launched by different companies under different names such as Phoenix/Hilux/Hilux-PNX (Hoya), Trilogy (Younger), Trexa/NXT/Aris (Essilor). Trivex lenses are made of polyurethane. It has optical quality; lightweight and safety features and it takes its name from these three features. They are also lighter than CR-39 and Polycarbonate [2, 6].

The sensitivity of eyes to ionizing radiation has attracted attention in the last decade. The International Radiological Protection Commission (ICRP), in its statement on tissue reactions in 2011, recommended that the eyepiece equivalent dose limit be lowered from 150 to 20 mSv for occupational exposure in cases of planned exposure [7]. In the beginning of 2018, this limit was implemented in national legislation in all European member states. While implementing this legislation, the Netherlands Commission on Radiation

[a] e-mail: mkamslioglu@bandirma.edu.tr (corresponding author)

Published online: 24 January 2023

Dosimetry (NCS) stated in its report that a number of issues related to the interpretation of certain terminology and protection of the lens (e.g. what level of eyepiece exposure? What is an "adequate system for monitoring"? Which groups of workers are expected to be involved? etc.) should be addressed. This report, which deals with the level of exposure (annual) considered "significant" to the lens of the eye, includes the International Atomic Energy Agency (IAEA) [8], International Organization of Standardization (ISO) [9] and the International Radiation Protection Association (IRPA) [10] reported that they recommend routine monitoring above 5 or 6 mSv per year and set the equivalent dose limit for the population at 15 mSv per year [11]. These radiation dose limits for the eye can also vary depending on use cases using spectacle lens. In addition, it is obvious that radiation protection properties will differ in people who spectacle lens depending on the type of spectacle lens. Nuclear radiation protection properties of spectacle lenses used in this study were calculated for photon, proton (H^{1}) and alpha (He^{+2}) particles.

Apart from the use of the spectacle lenses mentioned above in the routine treatment of the eyes, the effect of using daily spectacle on people with coronavirus disease 2019 (COVID-19) was investigated by Zeng et al. In the mentioned study, 276 patients admitted to the hospital with laboratory-confirmed COVID-19 in Hubei Province, China at the onset of the pandemic were evaluated. They reported that among these patients, those who reported wearing spectacle regularly for more than 8 h a day were lower than the general population. They concluded that wearing glasses for more than 8 h a day may protect them against SARS-CoV-2 infection [12].

In recent years, scientists have used simulation methods to determine the radiation-shielding properties of materials. Monte Carlo simulations are the most powerful methods used in these calculations. In this method, the transport of gamma-ray photons is simulated and their interaction with the material is investigated. Examples of Monte Carlo codes are MCNP6.2 [13], FLUKA [14], Geant4 [15], PENELOPE [16]. The ease of use and rich libraries of these codes ensure that the research results are consistent.

In the literature, it has been clearly stated that Monte Carlo codes can be applied by modeling in the investigation of radiation shielding parameters of materials and absorbed doses in tissues. Many studies have been reported in this context [17–22].

Radiation protection properties such as mass attenuation coefficient (MAC), half value layer (HVL), tenth value layer (TVL), mean free path (MFP), effective atomic number (Z_{eff}), effective electron density (N_{eff}) and equivalent atomic number (Z_{eq}) were determined using gamma rays in the energy range of 0.015–15 MeV. Gamma rays lose energy when interacting with a matter, and this situation is explained as three main events. These are the Photoelectric Effect (PE) that is predominant in the low energy range (~0.01–0.5 MeV), Compton Scattering (CS) that is predominant in the medium energy range (~0.1–10 MeV), and Pair Production (PP) that is dominant in the high energy range (~1.02 MeV) [23, 24]. In order to explain the interactions of gamma rays with matter, the MAC, HVL, TVL, MFP, Z_{eff}, N_{eff} and Z_{eq} of each lens used in the study were calculated. The theoretical results were obtained using the WinXCOM program and their accuracy was achieved with the results obtained using MCNP-6.2 Monte Carlo code. Gamma-ray transmission factors (TF) were calculated with MCNP-6.2. In addition, the range (PR) and the mass stopping power (MSP) values predicted in the energy range of 0.01–10 MeV for Proton (H^{1}) and alpha (He^{+2}) particles were calculated using the Stopping and Range of Ions in Matter (SRIM) code. SRIM is very popular in the ion implantation research and technology community and used widely in other branches of radiation material science. The source used in SRIM emits a single energy ion beam which interacts with the target atoms. In this study, the energies used for the ion beam are from 0.01 to 10 MeV. Mass stopping power tell us how energy is transferred to medium from charged particles. You can choose the ion, element and energy range for your desired target also it is a flexible software program. Finally, all results obtained were also compatible with Phy-X/PSD software [25].

2 Materials and methods

The radiation protection potential of the polymer structures of the glasses used in spectacle lens is expected to be excellent because of direct contact with the human. In this study, the radiation protection properties of spectacle lens (CR-39, Polycarbonate, Trivex) were investigated. The reason for examining CR-39, Polycarbonate and Trivex spectacle lenses in this study is that they are one of the more preferred lens types than mineral lenses [26, 27]. The reasons why PC and Trivex lenses are preferred by spectacle wearers include that they are lighter, more durable and have good natural UV protection properties compared to other lenses. CR-39 lenses are the most basic form of plastic lenses, and the abbe value is the highest, which means that the optical quality is the best. The disadvantage of these lenses is that they are easy to scratch. However, this situation can be eliminated by scratch-resistant coatings the lens [27, 28]. The properties of spectacle lenses are given in Table 1 [2, 3, 6, 29–31].

2.1 Monte Carlo simulations and nuclear radiation protection properties

MCNP-6.2 Monte Carlo Code [13] is a simulation program widely used by researchers in many fields such as nuclear physics, high energy physics, accelerator physics, and medical physics. In the literature, there are studies in which the radiation protection properties of MCNP-6.2 (Monte Carlo N-Particle Transport Code System-6.2 version) code are evaluated in many types of materials such as alloys, glass materials, additive concretes, and orthopedic medical materials. [32–36]. In this study, in order to compute the radiation attenuation parameters of spectacle lenses the energy range is 0.356–1.33 MeV, which is the frequently used energy range for MAC values, was used. The radiation source is defined as a point isotropic source. In the cell and surface cards where

Table 1 The properties of spectacle lenses

Lens name (material)	Refractive index	Abbe number	Density (g cm^{-3})	Chemical formula	Elemental composition (wt%)
CR-39 (Allyl diglycol carbonate)	1.49	58	1.32	$C_{12}H_{18}O_7$	0.52551 C 0.06615 H 0.40834 O
Polycarbonate (Bisphenol A)	1.59	31	1.20	$C_{16}H_{14}O_3$	0.75575 C 0.05549 H 0.18876 O
Trivex (Polyurethane)	1.53	43–45	1.11	$C_{11}H_{18}N_2$	0.74110 C 0.10176 H 0.15714 N

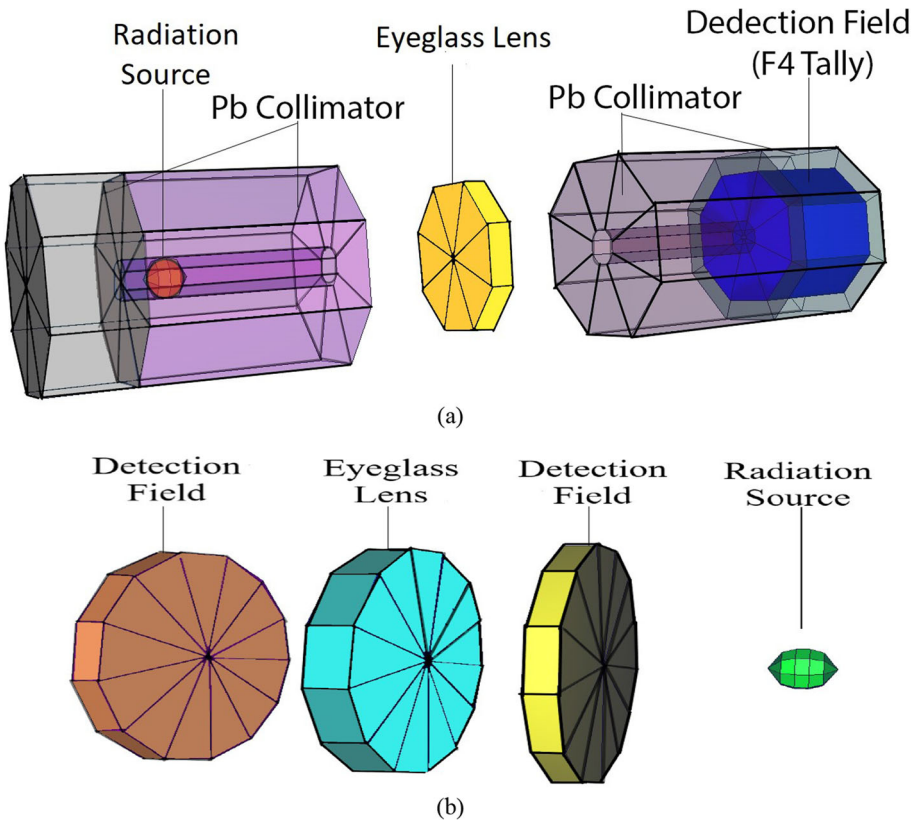

Fig. 1 Schematic views of **a** MAC and **b** TF setup achieved with MCNP6.2 simulation code (düzeltilecek)

material definitions are made in the simulation code, the elemental percentages and densities of the materials were used given in Table 1. The samples are positioned between the radiation source and the detector. The distance of the radiation source and the detector to the sample was set to 10 cm each. The photon from the radiation source travels to the detector after passing through the samples. Pb collimators have been used to cover the detector and the source as they prevent scattering. Different steps have been followed in computing these calculations. In the simulation setup, the photon flux that can pass through the material was measured by defining the F4 tally in the detector area and MAC calculations were obtained by using the data and Beer-Lambert Law. By comparing the MAC measurements and WinXcom [37] results, the simulation results were compared with the theoretical results, and R.D. values. Figure 1a shows the simulation setup prepared for MAC calculations. To calculate the transmission factor (I/I_0), it is necessary to measure the radiation flux entering and leaving the material. F4 tally was also defined in the detector fields in transmission simulations. Thus, the results were obtained by measuring the photon fluxes reaching and passing through the material. The simulation setup prepared in this direction is shown in Fig. 1b.

Information about the radiation protection parameters calculated in this study are given below. The decrease in energy because of the interaction of gamma rays with matter is exponential. This reduction is directly proportional to the thickness of the material

it passes through. Beer-Lambert law links the absorption of light in optics to the properties of the material through which it passes [38–41]. The MAC is obtained as in Eq. (2) using the Beer-Lambert law given in Eq. (1).

$$I = I_0 e^{-\mu x} \tag{1}$$

$$\mu_m = \frac{\mu}{\rho} \tag{2}$$

where μ (cm^{-1}) is the LAC value for the absorber, μ_m (cm^2g^{-1}) is the MAC value, x (cm) is the thickness of the material, ρ (g cm^{-3}) is the density of the absorber, I is the intensity of the beam after passing through the thickness x, I_0 is the intensity of the incident beam. In this study, the MAC value for the mixtures and components was calculated using the following Eq. (3) [42, 43].

$$\mu_m = \frac{\mu}{\rho} = \sum_i w_i \left(\mu/\rho\right)_i, \qquad w_i = n_i A_i \Big/ \sum_i n_i A_i \tag{3}$$

w_i is the fraction by weight of the ith constituent element, $(\mu/\rho)_i$ is the MAC of the ith element. A_i is the atomic weight of ith element and n_i is the number of elements in material.

Other basic theoretical parameters to explain the gamma ray protection efficiency of samples are: The HVL is the thickness of the material that reduces the incoming radiation intensity by half and absorbs 50% of the rays in the primary beam. The TVL is the thickness of the material that reduces the incident radiation intensity to one tenth. The MFP is the average move distance between two successive photon interactions [32, 44]. HVL, TVL and MFP can be calculated by Eq. 4–5–6, respectively.

$$\mathrm{HVL} = \frac{\ln 2}{\mu} \tag{4}$$

$$\mathrm{TVL} = \frac{\ln 10}{\mu} \tag{5}$$

$$\mathrm{MFP} = \frac{1}{\mu} \tag{6}$$

The cross section is the probability that any event occurring. Atomic cross section (σ_a) refers to the total photon interaction cross section per atom. The electronic cross section (σ_e) represents the total photon interaction cross section per electron. When the sample is a mixture or compound, the Z_{eff} is mentioned. The N_{eff} refers to the number of electrons per unit mass and is related to the effective atomic number. σ_a, σ_e, Z_{eff} and N_{eff} parameters are calculated by Eqs. 7–8–9–10, respectively [32, 45]. N_A is Avogadro's number (6.022×10^{23} mol^{-1}).

$$\sigma_a = \frac{\mu/\rho}{N_A \sum_i \frac{w_i}{A_i}} \tag{7}$$

$$\sigma_e = \frac{1}{N_A} \sum_i \left(\sum_j \frac{f_j A_j}{A_j} \right) w_i \tag{8}$$

$$Z_{eff} = \frac{\sigma_a}{\sigma_e} = \frac{\sum_i f_i A_i \left(\mu/\rho\right)_i}{\sum_j f_j \frac{A_j}{Z_j} \left(\mu/\rho\right)_j} \tag{9}$$

where Z_j, A_j denote the atomic number and atomic weight of the jth component, respectively. f_i, f_j denote the fractional weight of the ith and jth elements, respectively.

$$N_{eff} = \frac{\mu_m}{\sigma_e} = \frac{N_A}{M} Z_{eff} \sum_i n_i \tag{10}$$

M is molecular weight.

The Z_{eq} is calculated by dividing the Compton partial mass attenuation coefficient by the total MAC. Equation (11) was used for the interpolation of Z_{eq} [18, 33]. Detailed calculation procedures can be found in many studies [46–48].

$$Z_{eq} = \frac{Z_1(\log R_2 - \log R) + Z_2(\log R - \log R_1)}{\log R_2 - \log R_1} \tag{11}$$

where R's are $(\mu_m)_{compton}/(\mu_m)_{total}$ ratio. Z_1 and Z_2 refer to the atomic numbers of the elements corresponding to the ratios of R_1 and R_2, respectively.

The speed at which charged particles lose energy passing through a material is called the linear stopping power of the material. Linear stopping power ($-$ dE/dx) of the mater is given by Eq. (12). Here, the electronic stopping power is due to the interaction

of the charged particle with atomic electrons in the material. The nuclear stopping power arises from the interaction of the charged particle with the nucleus of the atom. The minus sign means that the charged particle will lose its kinetic energy [42].

$$-\frac{\mathrm{d}E}{\mathrm{d}x} = S_{\text{electronic}} + S_{\text{nuclear}} \tag{12}$$

For charged particles, the stopping power increases as the particle velocity decreases. The classical expression describing the specific energy loss is known as the Bethe–Bloch formula and is given in Eq. (13). Stopping power is a function of the mass, charge, the velocity of the ion, atomic number and density of the material [42, 49].

$$-\frac{\mathrm{d}E}{\mathrm{d}x} = \frac{4\pi e^4 z^2}{m_0 c^2 \beta^2} NZ\left[\ln\frac{2m_0 c^2\beta^2}{I\left(1-\beta^2\right)} - \beta^2\right] \tag{13}$$

where z charge of the incident particle ($z = 1$ for p; $z = 2$ for α), N and Z are the number density and the atomic number of the absorbing atoms respectively, m_0 is the rest mass of the particle, and e is the electronic charge. I represent the average excitation potential of the absorber. According to Eq. (13), particles with the greatest charge will have the largest specific energy loss. For example, alpha particles will lose energy at a greater rate than protons of the same velocity, but at a lower rate than that of more charged ions. NZ represents the electron density of the absorber. Materials with high atomic numbers or high density will consequently have the greatest linear stopping power [42]. The MSP for the compound or mixtures is determined by Eq. (14) [49, 50].

$$\frac{1}{\rho}\frac{\mathrm{d}E}{\mathrm{d}x} = \sum_i w_i \frac{1}{\rho_i}\left(\frac{\mathrm{d}E}{\mathrm{d}x}\right)_i \tag{14}$$

where $(\mathrm{d}E/\mathrm{d}x)$ is the stopping power of the ith element.

The distance that charged particles travel before losing all their energy in their interactions with matter is called the projected range (PR) or stopping distance of the particle and is given by Eq. (15). PR depends on the type of material, particle type and energy [49].

$$R = \int_0^E \frac{\mathrm{d}E}{\left(\mathrm{d}E/\mathrm{d}x\right)_{\text{electronic}} + \left(\mathrm{d}E/\mathrm{d}x\right)_{\text{nuclear}}} \tag{15}$$

MSP and PR values were calculated for H^{1} and He^{+2} particles using the Stopping and Range of Ions in Matter (SRIM) code. SRIM code is a software program that examines the interaction of ions with the matter [18, 51].

3 Results and discussion

The gamma protection parameters of spectacle lenses used in this study were calculated at energy range between 0.015 and 15 MeV. Some MAC values obtained using MCNP-6.2 simulation code and WinXCOM software are given in Table 2. The relative differences (RD) between the MAC values in Table 2 are calculated using Eq. (16). The RD values vary between 0.0561 and 1.219% for CR-39, 0.1584–2.572% for Polycarbonate and 0.001–6.479% for Trivex. As can be seen, the simulation results are very close to the calculation results. In this case, it is seen that the MAC values obtained from MCNP-6.2 and WinXCOM show a good agreement.

It is seen that the amount of radiation absorbed by the material decreases in the high-energy region studied. Although the MAC values obtained for spectacle lenses show similar behavior according to the change of energy, Trivex lenses have the highest MAC value in all gamma-ray energies.

$$\mathrm{RD} = \left|\left(\frac{(\mu/\rho)_{\text{WinXCOM}} - (\mu/\rho)_{\text{MCNPX}}}{(\mu/\rho)_{\text{WinXCOM}}}\right)\right| \times 100 \tag{16}$$

Figure 2 shows the total mass attenuation coefficient (μ_m) of the present lenses used. As can be seen from Fig. 2, μ_m values tend to decrease as the energy increases. Because there are different interactions of photons with matter. These interactions are known as PE, CS, and PP, and as the energy values increase, the PE decreases, while the PP effect increases and the CS effect does not change significantly [50]. The photoelectric effect occurs in electrons with high binding energies (especially the K shell). High binding energy decreases for low Z elements. Thus, the PE is reduced for low Z's. The main reason for this is the conservation of momentum. Above high binding energy, low cross sections cause sudden decreases in μ_m in this region [49]. In the energy range of 0.01–0.05 MeV, it was observed that CR-39 lenses were more dominant than other lenses and μ_m values varied between 0.2076 and 1.199 $\mathrm{cm^2 g^{-1}}$. CS refers to the collision of a photon with a weakly bonded electron [52]. Furthermore, CS predominates between approximately 0.1–10 MeV. In this region, the change of μ_m is slower than energy. It was observed that in the 0.1–10 MeV energy range, Trivex lenses were more dominant than other lenses and μ_m values varied between 0.021 and 1.166 $\mathrm{cm^2 g^{-1}}$. PP, at energies above 1.2 MeV is closely related to momentum conservation [52]. The probability of PP occurring is the only event that varies slightly with Z and increases with photon energy, unlike the Photoelectric and CS effect. So it is important to know that PP increases

Table 2 MCNP-6.2 and WinXCOM data comparison for MACs (cm^2g^{-1}) of spectacle lenses for different gamma-ray energies

Mass attenuation coefficient (μ_m) ($cm^2\ g^{-1}$)						
Investigated Lenses	Energy (MeV)					
	0.356	0.511	0.662	1.173	1.275	1.33
CR-39						
MCNP6.2	0.106605	0.089066	0.082411	0.059289	0.058865	0.062685
WinXCOM	0.106528	0.089116	0.082222	0.060021	0.058730	0.062639
R.D	0.072281	0.056107	0.229865	1.219573	0.229865	0.073437
Polycarbonate						
MCNP6.2	0.105655	0.085942	0.081262	0.058990	0.057120	0.061061
WinXCOM	0.105430	0.088211	0.081391	0.059413	0.058136	0.062010
R.D	0.213412	2.572242	0.158494	0.711965	1.747626	1.530398
Trivex						
MCNP6.2	0.107764	0.092000	0.085043	0.061072	0.060684	0.068876
WinXCOM	0.109947	0.091999	0.084896	0.061969	0.060635	0.064685
R.D	1.985502	0.001087	0.173153	1.447498	0.080811	6.479091

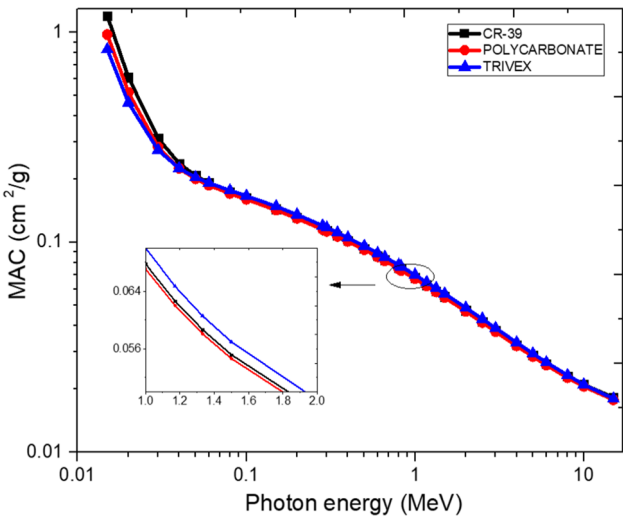

Fig. 2 The mass attenuation coefficient for the investigated CR-39, Polycarbonate and Trivex Lenses

with photon energy and Z [50]. Above 10 MeV, it was observed that CR-39 lenses were more dominant than other lenses and μm values varied between 0.018 and 0.021 cm^2g^{-1}.

HVL, TVL and MFP values provide considerable information about photon interaction parameters. According to the samples examined in this study, the changes in HVL, TVL and MFP are shown in Figs. 3, 4 and 5. The variation of the HVL value for CR-39, Polycarbonate and Trivex lenses is given in Fig. 3. In Fig. 3, it is clear that at all energies the CR-39 lens should have less thickness than Polycarbonate and Trivex. For example, HVL values were 0.438, 0.591 and 0.751 cm for CR-39, Polycarbonate and Trivex lenses at 0.015 MeV, respectively, while at 10 MeV they were 25.029, 28.095 and 29.722 cm, respectively. The required material thickness is proportional to the increasing energy. Figure 4 shows the variation of the TVL values of the studied samples according to the photon energy. These values are very small in the low energy range. TVL values increase with increasing energy values [53]. Figure 4 shows that the CR-39 lens has the lowest TVL values and the Trivex lens has the highest TVL values. For example, TVL values are 1.455, 1.963 and 2.496 cm for CR-39, Polycarbonate and Trivex lenses at 0.015 MeV, respectively, while at 10 MeV it is 83.145, 93.328 and 98.734 cm, respectively. Similar to HVL values, as more photons will penetrate the material with increasing photon energy, thicker material is required to reduce the intensity of the radiation by one-tenth [43]. Figure 5 shows the variation graph of MFP values according to the density of the samples examined, and it is seen from the graph that as the density increases, MFP values decrease and MFP values increase with increasing energy at all densities. For example, MFP values are 0.632, 0.852 and 1.084 cm at 0.015 MeV for CR-39, Polycarbonate and Trivex lenses, respectively, while at 10 MeV it is 36.109, 40.532 and 42.880 cm, respectively. As the density of the material increases, the distance that the photon moves between successive interactions decreases. As a result, when the HVL, TVL and MFP graphs are evaluated together for the samples examined, it is clear that the change of these graphs changes inversely with the LAC values and the density of the material and changes in proportion to the increasing photon energy. The lower the HVL, TVL and MFP values, the higher the possibility of photon interaction with the

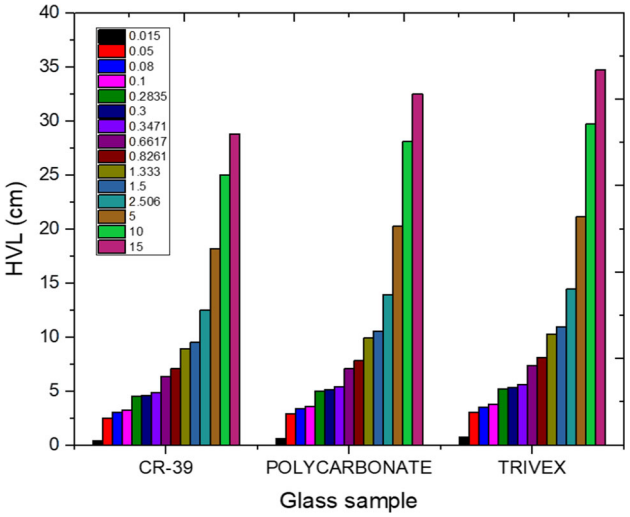

Fig. 3 The HVL for the investigated CR-39, Polycarbonate and Trivex Lenses

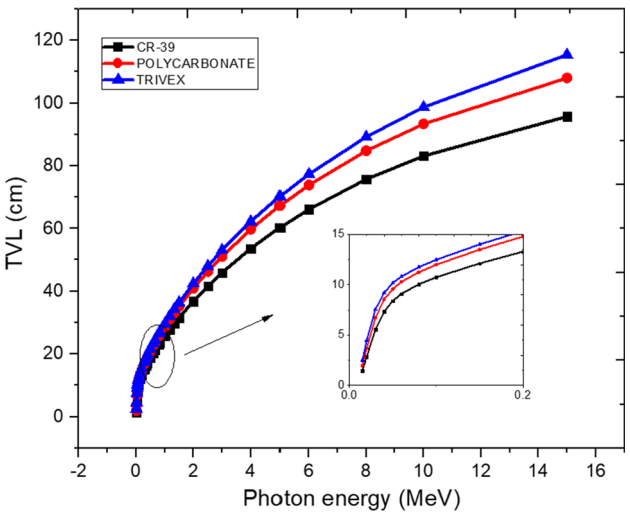

Fig. 4 The TVL for the investigated CR-39, Polycarbonate and Trivex Lenses

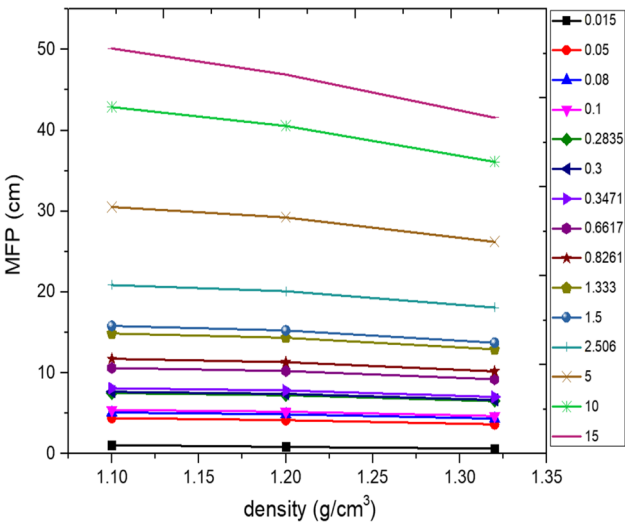

Fig. 5 The MFP for the investigated CR-39, Polycarbonate and Trivex lenses as a function of the density

material. In other words, low HVL, TVL and MFP values indicate that the material has superior photon attenuation. In this study, it was seen that the CR-39 lens, which has the minimum HVL, TVL and MFP at all energies, and the maximum density, has the best protection feature.

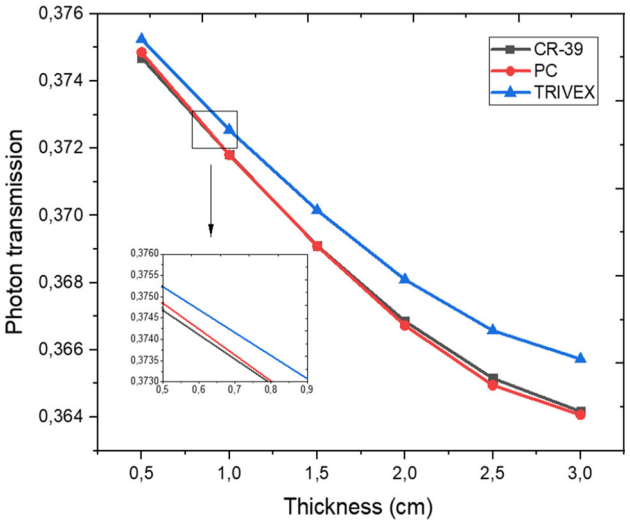

Fig. 6 Photon transmission for the investigated CR-39, Polycarbonate and Trivex Lenses

Table 3 Transmission photon flux (I) for spectacle lenses

Transmission photon flux (I) (for 1.25 MeV)			
Thickness (cm)	CR-39	Polycarbonate	Trivex
0.5	0.374689	0.374854	0.375239
1	0.371808	0.371800	0.372539
1.5	0.369100	0.369086	0.370157
2	0.366854	0.366728	0.368091
2.5	0.365157	0.364951	0.366577
3	0.364169	0.364070	0.365729

Transmission factor (TF) is the ratio of the intensity of radiation passing through a material to the intensity of incident radiation. The lower the TF value means that the more photons are weakened by the material and therefore the more protection it provides. As the thickness of the material increases, the TF value is expected to decrease[53]. In this study, the estimation of TF values depending on thickness at certain energies was made using the setup obtained from the MCNP-6.2 simulation program given in Fig. 1a. Figure 6 shows the variation of TF values obtained for each lens with thickness. In Fig. 6, thickness-dependent change of TFs at 1.25 MeV energy is given. In Fig. 6, it is seen that TFs decrease with increasing thickness. Because the TF values change depending on the chemical composition and density of the material as in the previous radiation protection parameters. At 1.25 MeV photon energy, it was observed that the Trivex lens had the highest TF value and the Polycarbonate lens had the lowest TF value in all thicknesses examined. Here the increased thickness showed once again proportional to the attenuation ability. Table 3 lists all TFs calculated for the lens materials used in this study.

The Z_{eff} is a measure of the average number of electrons of the material actively participating during the interaction, and no composite material can be symbolized by a single Z_{eff} as the interaction processes basically depend on atomic number and energy [54]. This means that photon attenuation in composite materials, as in elements, cannot be expressed by a single atomic number over the entire energy range, and the effective atomic number is not constant. Z_{eff} also depends on the atomic composition of the mixture [55]. Higher Z_{eff} gives a greater gamma-ray stopping power, i.e. the ability to absorb the energy of the impinging gamma radiation [56]. Figure 7 shows the change of Z_{eff} according to the photon energy. As can be clearly seen from Fig., the Z_{eff} values for each lens initially decrease with increasing energy, then remain constant and eventually increase slowly again. A decrease in Z_{eff} values below 0.3 MeV initially indicate that the photoelectric process is dominant in this range. The Z_{eff} values remaining constant between 0.4 and 2 MeV indicates that the Compton process is dominant in this range. The slow increase of Z_{eff} values above 2 MeV indicates that the pair production process is now dominant. In short, variations in Z_{eff} occur due to different photon interactions in low, medium and high-energy regions. All variations are related to the dependence of the total atomic cross section on the atomic number (Z). Photoelectric effect absorption cross section gives more weight to higher atomic number compounds than CS and PP. PE absorption section Z^4, which is dominant in the low energy range, is dependent on the CS section Z, which is dominant in the medium energy range, and the pair production section Z^2, which is dominant at high energies. Here, PE absorption becomes by far the most important interaction process. Therefore, Z_{eff} has reached its maximum value in the Photoelectric region. Z_{eff} remained constant at medium energies and increased slowly at high energies due to its lower cross section than the photoelectric cross section, but smaller than that of the lower energy range [57–59]. Among the lenses examined, the material with the lowest Z_{eff} value at all energies is Trivex. N_{eff}'s photon interaction mechanisms with Z_{eff} have the same qualitative energy dependence. The change of N_{eff}

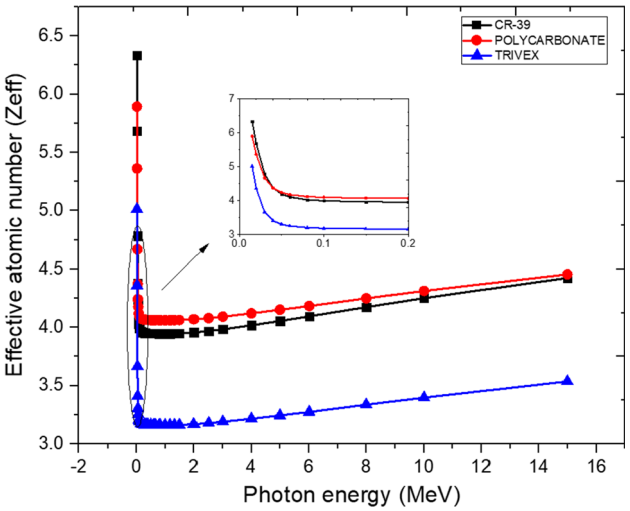

Fig. 7 The effective atomic number for the investigated CR-39, Polycarbonate and Trivex Lenses

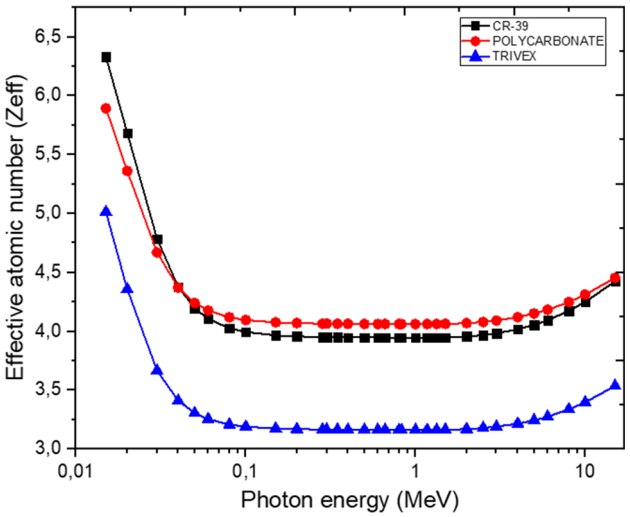

Fig. 8 The N_{eff} for the investigated CR-39, Polycarbonate and Trivex Lenses

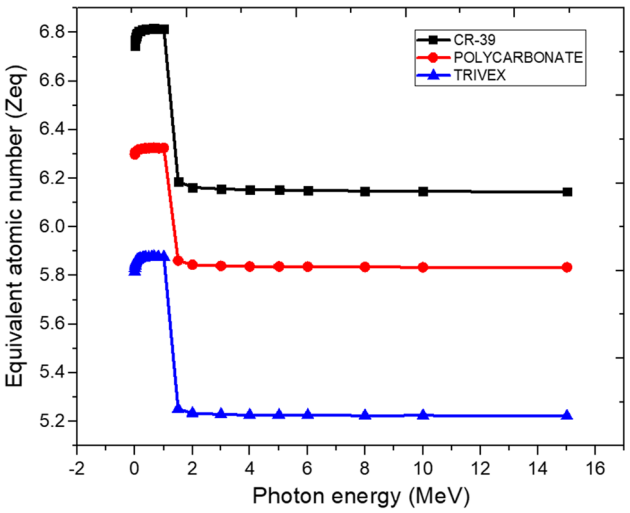

Fig. 9 The Z_{eq} for the investigated CR-39, Polycarbonate and Trivex Lenses

values given in Fig. 8 is inversely but closely related to Z_{eff}. In addition, the variation of the equivalent atomic number (Z_{eq}) values for the materials as a function of photon energy is presented in Fig. 9. The difference from Z_{eff}, which is related to the scattering and absorption processes of Z_{eq}, is that it is not related to the absorption process. In addition, while Z_{eff} reaches the highest values in the region where PE is dominant, it reaches the highest values in the region where Z_{eq} CS is dominant [25]. The highest and lowest Z_{eq} values for the CR-39, Polycarbonate and Trivex lenses, respectively, ranged from 6.145–6.817, 5.834–6.326 and 5.222–5.878.

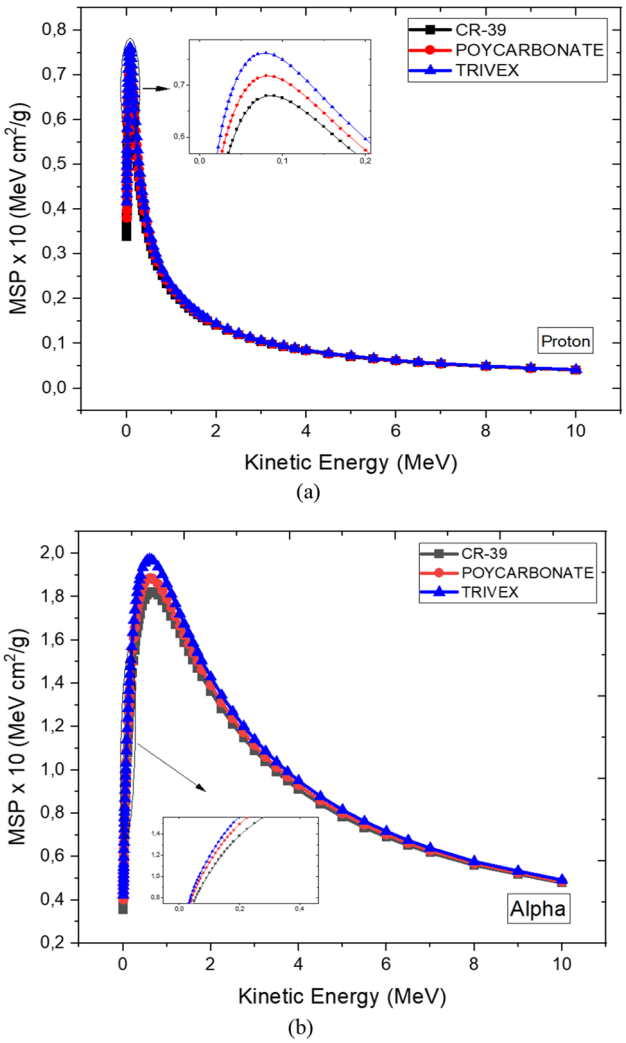

Fig. 10 Variation of **a** proton and **b** alpha MSP for the investigated CR-39, Polycarbonate and Trivex Lenses

In addition to the photon attenuation properties of the Spectacle lenses used in this study, particle (proton and alpha) absorption properties were also analyzed. The change of proton (H^1) and alpha (He^{+2}) particle stopping power (MSP) for Spectacle lenses is given in Fig. 10a, b. All the MSP values were obtained using SRIM software at energies between 0.010 and 10 MeV. As seen in Fig. 10a, b, MSP values initially reach a maximum with increasing kinetic energy and then decrease. It appears that the energy loss in alpha MSP change is greater than the proton MSP. Because alpha has a higher charge than a proton, it will cause more specific energy loss in the interaction [31, 37]. In Fig. 10a, b, it was seen that the Trivex lens has the largest MSP value at all energies and these values are in the range of 0.0415–0.07620 and 0.4229–1.973 for proton and alpha, respectively. The difference in MSP values is that this parameter depends on many properties such as the mass of the ion, its charge, speed, the atomic number and density of the material [42, 49]. The fact that charged particles lose their energy in a material be suggestive of question of how long these particles will penetrate before they lose all their energy. The projected range (PR) of the particle gives this amount. PR determines the distance or depth at which the particle of interest can penetrate into the material, so it is very important to determine the effective protective material. PR will increase with the increasing energy of the penetrating particle. A low PR value indicates that the material is highly radiation protection. In Fig. 11a, b, the change of proton and alpha PR values depending on kinetic energy is given. PR, like MSP, was obtained using SRIM software at energies between 0.010 and 10 MeV. In Fig. 11a, b, it is seen that the CR-39 lens has the lowest PR value compared to the other lenses at all energies and these values are in the range of 0.2404–1050 μm, 0.1546–96.87 μm for proton and alpha, respectively. This shows that the proton and alpha attenuation feature is the best in the CR-39 lens. These differences are due to the fact that PR depends on many variables (type of material, particle type and energy, etc.) such as MSP [49].

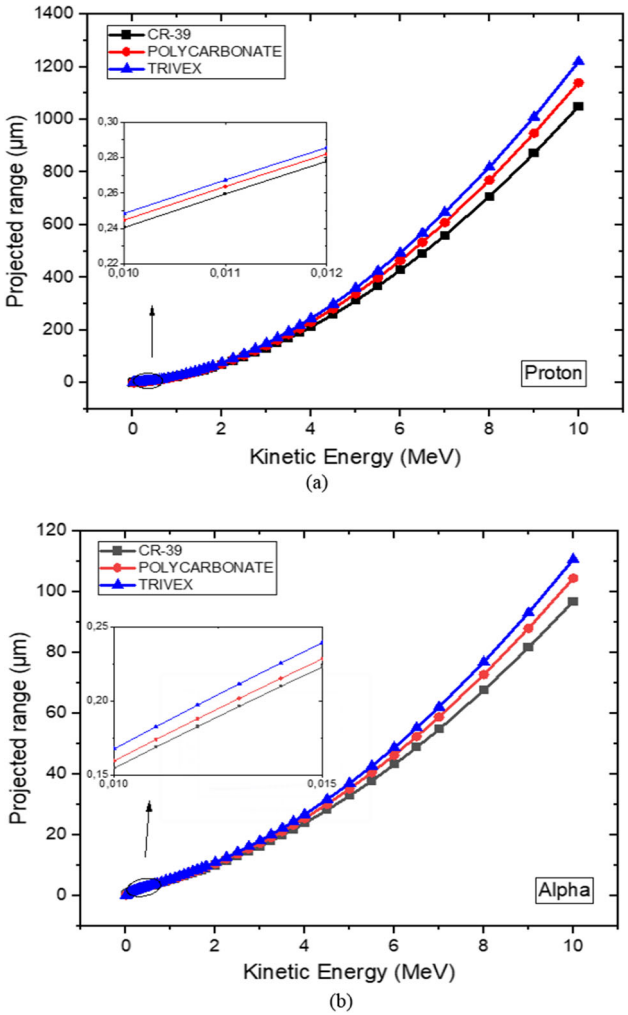

Fig. 11 Variation of **a** proton and **b** alpha projected range (PR) for the investigated CR-39, Polycarbonate and Trivex Lenses

4 Conclusions

In this study, the photon attenuation properties of spectacle lenses (CR-39, Polycarbonate, Trivex), as well as particle (proton and alpha) absorption properties were investigated. Thus, the radiation protection properties of each lens were interpreted both in different energy regions and for different types of radiation (photon, proton and alpha). In previous studies, the radiation protection properties of CR-39, Polycarbonate and Trivex lenses were not compared in this way. Therefore, this study will contribute to the literature in terms of providing detailed information about the radiation protection parameters of the researched lenses. The results obtained from the study are as follows:

- It was observed that the CR-39 lens had the highest MAC values at low and high energies, while the Trivex lens had the highest MAC values at medium energies.
- It was seen that the CR-39 lens had minimum HVL, TVL and MFP values at all energies. This means that the CR-39 lens has better photon attenuation than Polycarbonate and Trivex lenses.
- The Trivex lens had the highest TF value and the Polycarbonate lens had the lowest TF value. Thus, it has been observed that Trivex has the least protection properties among lenses.
- While the maximum Z_{eff} value was obtained in the region where the photoelectric interaction is dominant, the maximum N_{eff} value was observed in the region where Compton scattering was dominant.
- The Trivex lens had the largest proton and alpha MSP values at all energies. In order to make MSP more significant, proton and alpha PR values were calculated. In all energies, it was observed that the Trivex lens had the highest PR value and the CR-39 lens had the lowest PR value. This shows that the proton and alpha protection properties are the best in the CR-39 lens.
- The amount of radiation that can be exposed varies according to the structure of the Spectacle lens material used. In the literature, it has been shown that the radiation shielding properties of some glass increase due to the increase in the ratio of bismuth in the glass content [17, 20]. However, the results obtained showed that there should be a tendency to conduct similar studies for the lens material.

Data Availability Statement No Data associated in the manuscript.

References

1. WHO, World report on vision. World health Organization. https://apps.who.int/iris/handle/10665/328717. Accessed 12 Jan 2021 (2019)
2. J. Alonso, J.A. Gómez-Pedrero, J.A. Quiroga, *Modern Ophthalmic Optics* (Cambridge University Press, 2019)
3. S. Musikant, *Optical Materials: An Introduction to Selection and Application* (CRC Press, 1985)
4. F. Şen, B.G. Durdu, M. Oduncuoğlu et al., A theoretical investigation by DFT method on CR-39 monomer that is a plastic polymer commonly used in the manufacture of eyeglass lenses. Am. J. Opt. Photonics **2**, 7–11 (2014)
5. J. Miller, B. Kislin, Colonel, et al., *Policarbonate Versus CR-39 Lenses: A Field Study, SCHOOL OF AEROSPACE MEDICINE BROOKS AFB TX.* (1979)
6. B. Ralph Chou, S.J. Dain, B.B. Cheng, Effect of ultraviolet exposure on impact resistance of ophthalmic lenses. Optom. Vis. Sci. **92**, 1154–1160 (2015)
7. ICRP, *Dose Limits to the Lens of the Eyes: New Limit for the Lens of the Eye—International Basic Safety Standards and related guidance* (2013)
8. IAEA-TECDOC, Implications for occupational radiation protection of the new dose limit for the lens of the eye. Int. At. Energy Agency **1731** (2013)
9. ISO, *IRPA Guidance on Implementation of Eye Dose Monitoring and Eye Protection of Workers* (2015)
10. IRPA, *IRPA Guidance on Implementation of Eye Dose Monitoring and Eye Protection of Workers* (2017)
11. NCS, *Guidelines for Radiation Protection and Dosimetry of the Eye Lens* (2018)
12. W. Zeng, X. Wang, J. Li et al., Association of dailywear of eyeglasses with susceptibility to coronavirus disease 2019 infection. JAMA Ophthalmol. **138**, 1196–1199 (2020)
13. J.S. Hendricks, G.W. Mckinney, M.L. Fensin, et al., MCNPX 2.6.0 Extensions. Work 73. http://mcnpx.lanl.gov. Accessed 19 March 2020 (2008)
14. F. Ballarini, G. Battistoni, M. Brugger, M. Campanella, M. Carboni, F. Cerutti et al., The physics of the FLUKA code: recent developments. Adv. Sp. Res. **40**, 1339–1349 (2007)
15. S. Agostinelli, J. Allison, K. Amako, J. Apostolakis, H. Araujo, P. Arce et al., GEANT4—a simulation toolkit. Nucl. Instrum. Methods Phys. Res. Sect. A Accel. Spectrom. Detect. Assoc. Equip. **506**, 250–303 (2003)
16. F. Salvat, J. Fernández-Vera, J. Sempau, PENELOPE-2008: a code system for Monte Carlo simulation of electron and photon transport (2009)
17. A.M.A. Mostafa, H.M. Zakaly, M. Pyshkina, S.A. Issa, H.O. Tekin et al., Multi-objective optimization strategies for radiation shielding performance of BZBB glasses using Bi_2O_3: a FLUKA Monte Carlo code calculations. J. Mater. Res. Technol. **9**(6), 12335–12345 (2020)
18. M. Kamislioglu, Research on the effects of bismuth borate glass system on nuclear radiation shielding parameters. Results Phys. **22**, 103844 (2021)
19. G. Susoy, E.A. Guclu, O. Kilicoglu, M. Kamislioglu, M.S. Al-Buriahi, M.M. Abuzaid, H.O. Tekin, The impact of Cr_2O_3 additive on nuclear radiation shielding properties of LiF–SrO–B_2O_3 glass system. Mater. Chem. Phys. **242**, 122481 (2020)
20. A.M. Madbouly, O.I. Sallam, S.A. Issa, M. Rashad, A. Hamdy, H.O. Tekin, H.M. Zakaly, Experimental and FLUKA evaluation on structure and optical properties and γ-radiation shielding capacity of bismuth borophosphate glasses. Prog. Nucl. Energy **148**, 104219 (2022)
21. B. Güçlü, E.E. Altunsoy, T. Manici, H.O. Tekin, Effect of humeral locking plate system on absorbed energy in breast tissue with different radiological energies using MCNPX code. J. Test. Eval. **49**(1), 329–337 (2019)
22. H.M. Zakaly, H.A. Saudi, S.A. Issa, M. Rashad, A.I. Elazaka, H.O. Tekin, Y.B. Saddeek, Alteration of optical, structural, mechanical durability and nuclear radiation attenuation properties of barium borosilicate glasses through BaO reinforcement: Experimental and numerical analyses. Ceram. Int. **47**(4), 5587–5596 (2021)
23. D.K. Gaikwad, P.P. Pawar, T.P. Selvam, Mass attenuation coefficients and effective atomic numbers of biological compounds for gamma ray interactions. Radiat. Phys. Chem. **138**, 75–80 (2017)
24. A.S. Abouhaswa, H.M.H. Zakaly, S.A.M. Issa et al., Synthesis, physical, optical, mechanical, and radiation attenuation properties of TiO_2–Na_2O–Bi_2O_3–B_2O_3 glasses. Ceram. Int. **47**, 185–204 (2021)
25. E. Şakar, Ö.F. Özpolat, B. Alım et al., Phy-X/PSD: development of a user friendly online software for calculation of parameters relevant to radiation shielding and dosimetry. Radiat. Phys. Chem. **166**, 108496 (2020)
26. R. Chantarachindawong, T. Osotchan, P. Chindaudom, T. Srikhirin, Hard coatings for CR-39 based on Al_2O_3–ZrO_2 3-glycidoxypropyltrimethoxysilane (GPTMS) and tetraethoxysilane (TEOS) nanocomposites. J. Sol–Gel Sci. Technol. **79**, 190–200 (2016)
27. R. Pillay, R. Hansraj, N. Rampersad, Historical development, applications and advances in materials used in spectacle lenses and contact lenses. Clin. Optom. **12**, 157–167 (2020)
28. M.L. Rubin, Spectacles: past, present, and future. Surv. Ophtalmol. **30**(5), 312–327 (1986)
29. B.R. Chou, J.K. Hovis, Effect of multiple antireflection coatings on impact resistance of Hoya Phoenix spectacle lenses. Clin. Exp. Optom. **89**, 86–89 (2006)
30. A.K. Bhootra, *Ophthalmic Lenses* (Jaypee Brothers Medical Publishers, 2009)
31. J. Fernando, R. Domínguez, Resistencia a los impactos: una mirada óptica. Cienc. Tecnol. Salud Vis. Ocul. **11**, 113–125 (2013)
32. M. Kamislioglu, E.E. Altunsoy Guclu, H.O. Tekin, Comparative evaluation of nuclear radiation shielding properties of $x$$TeO_2$ + (100–x)Li_2O glass system. Appl. Phys. A Mater. Sci. Process. (2020). https://doi.org/10.1007/s00339-020-3284-3
33. Ö. Akçalı, M. Çağlar, O. Toker et al., An investigation on gamma-ray shielding properties of quaternary glassy composite ($Na_2Si_3O_7$/Bi_2O_3/B_2O_3/Sb_2O_3) by BXCOM and MCNP 62 code. Prog. Nucl. Energy **125**, 103364 (2020)
34. M. Çağlar, H. Kayacık, Y. Karabul et al., $Na_2Si_3O_7$/BaO composites for the gamma-ray shielding in medical applications: experimental, MCNP5, and WinXCom studies. Prog. Nucl. Energy **117**, 1–11 (2019)
35. C.M. Salgado, L.E.B. Brandão, R. Schirru et al., Validation of a NaI(Tl) detector's model developed with MCNP-X code. Prog. Nucl. Energy **59**, 19–25 (2012)
36. L. Gerward, N. Guilbert, K.B. Jensen, H. Levring, WinXCom—a program for calculating X-ray attenuation coefficients. Radiat. Phys. Chem. **71**, 653–654 (2004)
37. B.R. Kerur, S.R. Thontadarya, B. Hanumaiah, A novel method for the determination of x-ray mass attenuation coefficients. Int. J. Radiat. Appl. Instrum. Part **42**, 571–575 (1991)
38. F. Mazda, Optics and vision, in *Telecommunications Engineer's Reference Book* (1993), pp. 328–360
39. G.K. Skinner, Practical gamma-ray spectrometry, Spectrochim. Acta Part A Mol. Biomol. Spectrosc. (2008)
40. M. Bass, J.M. Enoch, L. Vasudevan, *Handbook of Optics, Handbook of optics: volume I-geometrical and physical optics, polarized light, components and instruments. McGraw-Hill Education.* (McGraw-Hill, New York, 2010)

41. J.H. Hubbell, S.M. Seltzer, Tables of X-ray mass attenuation coefficients and mass energy-absorption coefficients 1 keV to 20 MeV for elements Z = 1 to 92 and 48 additional substances of dosimetric ınterest (1995)
42. G.F. Knoll, *Radiation Detection and Measurement, John Wiley & Sons,* (Wiley, 2010)
43. P. Yasaka, N. Pattanaboonmee, H.J. Kim et al., Gamma radiation shielding and optical properties measurements of zinc bismuth borate glasses. Ann. Nucl. Energy **68**, 4–9 (2014)
44. M.W. Marashdeh, I.F. Al-Hamarneh, E.M. Abdel Munem et al., Determining the mass attenuation coefficient, effective atomic number, and electron density of raw wood and binderless particleboards of Rhizophora spp. by using Monte Carlo simulation. Results Phys. **5**, 228–234 (2015)
45. M.I. Sayyed, Y. Elmahroug, B.O. Elbashir, S.A.M. Issa, Gamma-ray shielding properties of zinc oxide soda lime silica glasses. J. Mater. Sci. Mater. Electron **28**, 4064–4074 (2017)
46. N. Ekinci, E. Kavaz, B. Aygün, U. Perişanoğlu, Gamma ray shielding capabilities of rhenium-based superalloys. Radiat. Eff. Defects Solids **174**, 435–451 (2019)
47. M.I. Sayyed, H.O. Tekin, O. Agar, Gamma photon and neutron attenuation properties of MgO–BaO–B_2O_3–TeO_2–Cr_2O_3 glasses: the role of TeO_2. Radiat. Phys. Chem. **163**, 58–66 (2019)
48. G. Susoy, E.E.A. Guclu, O. Kilicoglu et al., The impact of Cr_2O_3 additive on nuclear radiation shielding properties of LiF–SrO–B_2O_3 glass system. Mater. Chem. Phys. **242**, 122481 (2020)
49. W.R. Leo, D.G. Haase, *Techniques for Nuclear and Particle Physics Experiments* (Springer, New York, 1990)
50. N. Tsoulfanidis, S. Landsberger, *Measurement Detection of Radiation*, 4th edn. (Taylor & Francis Group, CRC Press, 2015)
51. M. Kamislioglu, An investigation into gamma radiation shielding parameters of the (Al:Si) and (Al + Na): Si-doped international simple glasses (ISG) used in nuclear waste management, deploying Phy-X/PSD and SRIM software. J. Mater. Sci. Mater. Electron **32**, 12690–12704 (2021)
52. C.W. Fabjan, S. Herwig, Particle physics reference library, in *Detectors for Particles and Radiation. Open access*, vol. 2, (Springer, 2020)
53. H.M. Zakaly, S.A. Issa, H.A. Saudi, G.A. Alharshan, M.A.M. Uosif, A.M.A. Henaish, Structure, Mössbauer, electrical, and γ-ray attenuation-properties of magnesium zinc ferrite synthesized co-precipitation method. Sci. Rep. **12**(1), 1–16 (2022)
54. M.V. Manjunatha, T.K. Umesh, Effective atomic number of some rare earth compounds determined by the study of external bremsstrahlung. J. Radiat. Res. Appl. Sci. **8**, 428–432 (2015)
55. P. Andreo, Calibration of photon and electron beams. Rev. Radiat. Oncol. Phys. A Handb. Teach. Stud. **24**, 301–354 (2005)
56. M.F. Lannunziata, Handbook of radioactivity analysis, in *Radiation Physics and Detectors*, vol. 1, (Academic Press, 2020)
57. S.R. Manohara, S.M. Hanagodimath, K.S. Thind, L. Gerward, On the effective atomic number and electron density: a comprehensive set of formulas for all types of materials and energies above 1 keV. Nucl. Instrum. Methods Phys. Res. Sect. B Beam. Interact. Mater. At. **266**, 3906–3912 (2008)
58. M. Kamışlıoğlu, Beton-PbO-WO_3 Bileşiği için İyonlaştırıcı Radyasyon Etkileşim Parametrelerinden Kütle Durdurma Gücü ve Durdurma Mesafesinin 0.015–20 MeV Enerji A ralığında Hesaplanması Ionizing Radiation Interaction Parameters Calculation of Mass Stopping Power and Pr. Eur. J. Sci. Technol. 786–795 (2020).
59. S. Stalin, D.K. Gaikwad, M.S. Al-Buriahi et al., Influence of Bi_2O_3/WO_3 substitution on the optical, mechanical, chemical durability and gamma ray shielding properties of lithium-borate glasses. Ceram. Int. **47**, 5286–5299 (2021)